مجلة جامعة بني وليد للعلوم الإنسانية والتطبيقية

تصدر عن جامعة بني وليد – ليبيا

Website: https://jhas-bwu.com/index.php/bwjhas/index

العدد التاسع والعشرون، 2023

Physico-mechanical and sulfate resistance evaluation of concrete made with ground granulated blast-furnace slag.

S. Attelisi[1*], M. Albgoul[2], M. Ebailila[3], A. Abdulla[4]

[1,2,3]Department of Civil Engineering/Faculty of Engineering/Bani Waleed University, Libya

[4]Department of Civil Engineering/ College of Technical Sciences Bani Waleed, Libya

*Crosspnding author: mansour.ebailila@yahh.co.uk

تاريخ الاستلام: 14-06-2023 تاريخ القبول: 30-06-2023 تاريخ النشر: 07-09-2023

Abstract: In recent years, with the aim of restricting the formation of ettringite and reducing the environmental impact associated with cement manufacturing, the incorporation of ground granulated blast-furnace slag (GGBS) as a partial replacement of cement has become a common tendency, due to its efficiency in enhancing the physico-mechanical properties of concrete. This research study reports the experimental results on the properties of concrete containing GGBS at different partial cement substitution levels (0, 50, and 75%). A total of three concrete mixes were manufactured using a water/cement ratio (w/c) of 0.55 and binder: sand: aggregate proportion of 1: 2: 3. Thereafter, a physico-mechanical evaluation including slump test, compactability degree test, unconfined compression strength (UCS) test, tensile splitting strength (TSS) test and sulfate attack, were performed to assess the concrete performance. The experimental results suggested that, although the use of GGBS as a partial cement replacement slightly affects the mechanical performance at the early curing age, its usage improves the consistency and yielded a higher residual mechanical performance after immersion in sulfate solution, particularly at higher substitution level (75%).

Keywords: (Ettringite, magnesium sulfate, mechanical strength, sodium sulfate, sulfate attack)

Introduction

Global warming is one of the substantial concerns for human civilization's future, imposing the necessity for the development of eco-friendly and sustainable construction strategies [1]. Generally, concrete is considered a widely versatile construction substance, probably due to its cost efficiency, its ability to be moulded into various shapes, and raw material availability [2]. Concrete is also rated as the second most utilized material globally, behind water [3], with an estimated usage of 30 million tons annually [1]. It is typically composed of binder, aggregates, sand, and water, of which Portland cement is the traditional binder used for binding the matrix. However, there have been some negative environmental and sustainability issues associated with the manufacturing of Portland cement. These included; 1) the use of a huge amount of natural raw materials especially limestone and clay (2.8 tons of raw materials per one ton of cement) [4]; 2) the enormous energy consumption (5000 MJ per one ton) [5]; and 3) the higher carbon dioxide gas emissions emitted to the atmosphere (one ton of CO_2 per one ton of cement), which represents 5 % of anthropic emissions in the world [6].

Apart from the environmental consequences, the development of concrete using Portland cement also show limited efficiency in the presence of sulfate, causing serious problematic issues including concrete crack, expansion, spalling, and deterioration, due to the formation of gypsum and ettringite

[7]. Ettringite is a hydrous calcium aluminate sulfate mineral that forms due to the reaction between the hydrated compounds (from cement hydration), sulfate (from cement or penetrated to concrete from an external source), and water [8]. This mineral has a higher water absorption capability [9,10], attracting water, growing in pore voids as a needle-shaped crystal, causing cracks, expansion and thus, softening the concrete matrix. Therefore, the use of industrial and agricultural by-products (pozzolans) such as rice husk ash-RHA (agricultural by-product), ground granulated blast-furnace slag-GGBS (an industrial by-product of steel manufacturing), and pulverized fly ash-PFA (a by-product of the coal-fired electric power station), has been encouraged [11]. This is due to the potential of these supplementary cementitious materials in enhancing the physico-mechanical properties of concrete through their pozzolanic reactions and filler effect, along with their beneficial impacts on preserving the environment [12].

GGBS, which is a latent hydraulic material produced as a by-product of the steel industry, is one of the superior cementitious materials, as this is an effective way of enhancing the sulfate resistance of concrete. In the literature, Yan et al., 2019 [7], for example, used GGBS as a partial replacement (0, 25, 50, and 75%) of cement, and reported that 50% replacement yielded a beneficial sulfate resistance under the standard curing, while 75% was the optimum amount for steam-cured specimens immersed in 5% sodium sulfate solution. Hadisadok et al., 2012 [13] investigated the effect of separate 5% sodium and 5% magnesium sulfate on concrete and suggested the use of more than 30% of low reactivity GGBS as a partial cement replacement for better sulfate resistance. El-Hachem et al., 2012 [14] concluded that mortar with lower water/cement (w/c) ratio is superior in sulfate resistance because it induces better permeability. Zhang et al., 2013 [15] studied the effect of a mixed solution of different sodium sulfate and chloride concentration, and concluded that the expansion of concrete was directly and adversely proportional to the sulfate and chloride concentration, respectively,
Given the above-mentioned literature, it is obvious that designing a concrete mix containing GGBS to restrict the sulfate attack, is possible. However, the relevant literature in terms of the effect of a binary solution of magnesium and sodium sulfate on the mechanical performance of concrete is still vague and insignificant. Therefore, an attempt has been made in this study to explore the effect of the binary solution of magnesium and sodium sulfate on the performance of concrete made with different proportions (0, 50 and 75%) of GGBS.

Methodology

1- Materials

The raw materials used in this research study included Portland cement (PC), ground granulated blast-furnace slag (GGBS), coarse aggregate (CA), fine aggregate (FA), deionized water, and binary sulfate solution. **Table 1** and **Table 2** summarize the oxide compositions and some physical characteristics for PC and GGBS, whereas **Fig.1** and **Fig.2** plot, respectively, the particle size distribution of the raw materials, and the thermogravimetric-TG and derivative thermogravimetric-DTG analysis for PC and GGBS.

Table 1: Oxide compositions of PC and GGBS.

Oxides	PC	GGBS
CaO	61.49	37.99
MgO	3.54	8.78
SiO_2	18.84	35.54
Al_2O_3	4.77	11.46
Na_2O	0.02	0.37
P_2O_5	0.1	0.02
Fe_2O_3	2.87	0.42
Mn_2O_3	0.05	0.43
K_2O	0.57	0.43
TiO_2	0.26	0.7
V_2O_5	0.06	0.04
BaO	0.05	0.09
SO_3	3.12	1.54
Loss on ignition	4.3	2

Table 2: Physical properties of PC and GGBS.

Oxides	PC	GGBS
Insoluble residue	0.5	0.3
Bulk density (kg/m^3)	1400	1200
Specific gravity (Mg/m^3)	3.15	2.9
Glass content	-	90
Blaine fineness (m^2/kg)	365	450
Alkalinity value (pH)	13.41	10.4
Colour	Grey	Off-white
Physical form	Powder	Powder

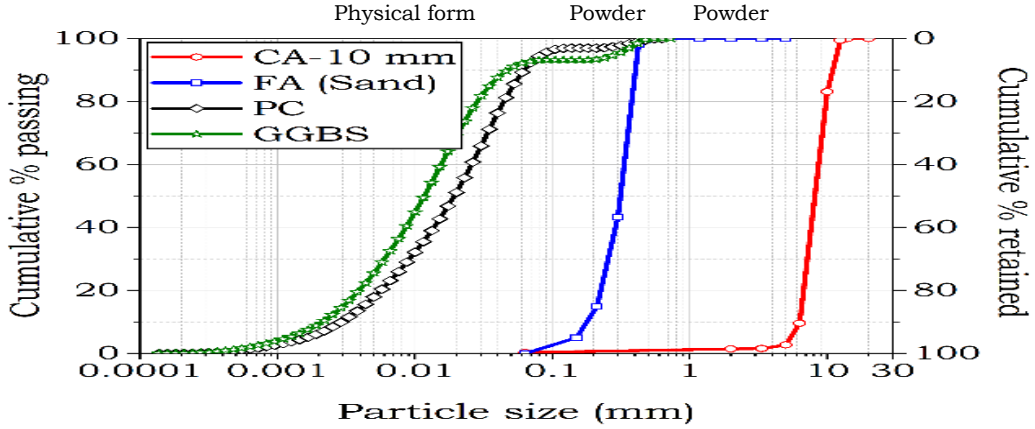

Fig. 1: Particle size distribution of the raw materials.

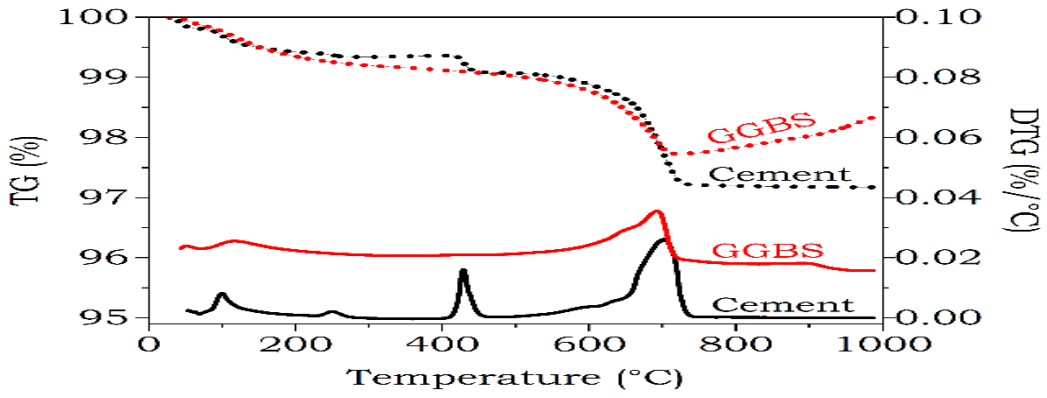

Fig. 2: TG (dotted lines) and DTG (solid lines) curves for PC and GGBS.

The PC used was a commercial Portland cement (CEM-I 42.5 N) in the form of grey fine powder. It was manufactured in compliance with the requirements of BS EN 197-1:2011 [16] and obtained from large

cement UK by a local contractor. The TG/DTG analysis of the un-hydrated CEM-I PC indicated a negligible mass loss of 2.8%, as the temperature increases up to 1000 ℃, which is represented in the DTG curve by three endothermic peaks. The first peak located in the range of 50-150 ℃ is due to the dehydration of gypsum, whereas the second peak at 400-450 ℃, and the third peak at 650-750 ℃, are due to the dihydroxylation of portlandite (calcium hydroxide) and the decomposition of calcite, respectively.

The GGBS utilized was a latent hydraulic pozzolan complied with BS EN 15167-1:2006 [17], and obtained from Civil and Marine Slag Cement Ltd, LIanwern, Newport, UK, by a local contractor. The TG curve (see **Fig. 2**) indicated that, as the temperature increases to 1000 ℃, the mass was reduced by 2.26%, which is represented in the DTG by a single peak at 550-700 ℃, owing to the calcite decomposition.

The coarse aggregate (CA) was a limestone in the grade of 10 mm, while fine aggregate (FA) is natural river sand from Bristol Channel. Both aggregates complied with BS EN 12620:2002+A1 [18] and were obtained from a local quarry through a local supplier.

The binary sulfate solution used was prepared by dissolving a total amount of 750g of an equal quantity of magnesium sulfate ($MgSO_4$) and sodium sulfate ($NaSO_4$) in 20 liters. Both magnesium and sodium sulfate were obtained from Fisher Scientific Ltd, UK, through a local supplier. As for the relatively higher sulfate concentration, it was adopted to accelerate the effect of sulfate on concrete, thus, the ease of identifying the benefit of GGBS in concrete.

2- Mix design and specimen preparation

The concrete mix compositions assessed under this study were designed using, 1) a fixed binder: sand: aggregate proportion of 1:2:3, 2) a w/c ratio of 0.55, and 3) three various binder combinations. These binders (see **Table 3**) were made of; 1) 100% of PC (as a control mix); 2) 50PC-50GGBS (M2), representing an intermediate cement replacement; and 3) 25PC-75GGBS (M3), representing a high cement replacement. The purpose was to obtain an eco-friendly concrete mix design, with a high sulfate resistance performance.

Table 3: Mix compositions of PC-based and GGBS-based concrete mixes.

Mix Design	PC	GGBS	W	FA	CA
M1 (100PC)	6	-	3.3	12	18
M2(50PC-50GGBS)	3	3	3.3	12	18
M3(25PC-75GGBS)	1.5	4.5	3.3	12	18

A total of 18 cubes (100 mm × 100 mm × 100 mm) and 6 cylinders (200 mm in height and 100 mm in diameter) were prepared in line with BS EN 206:2013+A2:2021 [19], BS EN 12350-1:2019 [20], and BS EN 12390-1:2021 [21], for all the concrete mixes. For each mix, the dry ingredients (PC, GGBS, CA and FA) were initially mixed in a mixer for 3 minutes, before the water was introduced and the mixing continued for further 3 minutes. Afterwards, the consistency of fresh concrete was measured, in accordance with the relevant standard. The semi-paste mixture was then poured into the pre-oiled moulds and vibrated for 1 minute to remove air voids. Thereafter, the concrete-filled moulds were stored at 20±2 ℃ to be de-moulded after 24 hours, preparing for the curing. Finally, 9 cubes and 3 cylinders were cured in a water tank at 20±2 ℃, while the remaining specimens were cured in a sulfate solution, until the date of testing.

3- Testing method

The designed concrete mixes were evaluated in terms of consistency (slump and compactability degree), mechanical properties (UCS and TSS), and sulfate resistance (variation in UCS and TSS). The slump and compactability degree tests were carried out in accordance with BS EN 12350-2:2019 [22] and BS EN 12350-4:2019 [23], respectively. The UCS test was conducted on three water-cured specimens per mix composition at each of the prescribed curing periods (7, 28 and 56 days), in line with BS EN 12350-3 2019 [24]. The TSS test was performed in accordance with BS EN 12350-6: 2009 [25] on three cylinders per mix composition at the end of 28 days of moist curing. As for the sulfate resistance, it was measured in terms of the variation in UCS and TSS of sulfate-cured specimens, relative to their water-cured counterparts.

Results and discussion

1- Consistency of fresh concrete

Fig. 3 presents the consistency results of concrete batches obtained from the slump test and compactability degree test.

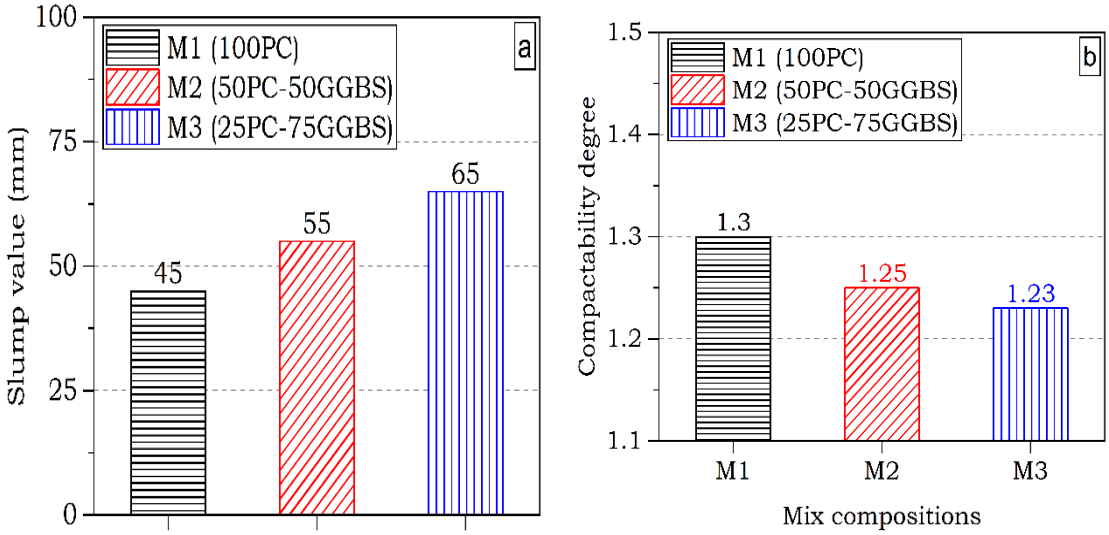

Fig 3: Consistency of fresh concrete; **a)** slump values, and **b)** compactability degree.

The results revealed a gradual increase in the slump value, as the quantity of GGBS increased, where the control concrete mix (M1; 100PC) exhibited the lowest slump (45 mm), relative to that of 55 and 65 mm for M2 (50PC-50GGBS) and M3 (25PC-75GGBS), respectively. This trend, however, was in reverse order in the case of the compactability degree (see **Fig. 3b**), proving the accuracy of the laboratory experiments. The improvement in the consistency due to GGBS is an indicator of reducing the water demand and improving the pumpability. In addition, the consistency was in line with the observation of several studies [26–30]. This enhancement is probably attributed to the smoothness of the GGBS, the poorer early hydration, the lower calcium oxide of the GGBS, and the lower water absorption capability of the GGBS-based system, compared to the cement-based system [26–30].

2- Strength development in water

2.1-UCS of concretes cured in water

Fig. 4 presents the unconfined compression strength development of all the formulated concretes over a prolonged ambient curing period of up to 56 days.

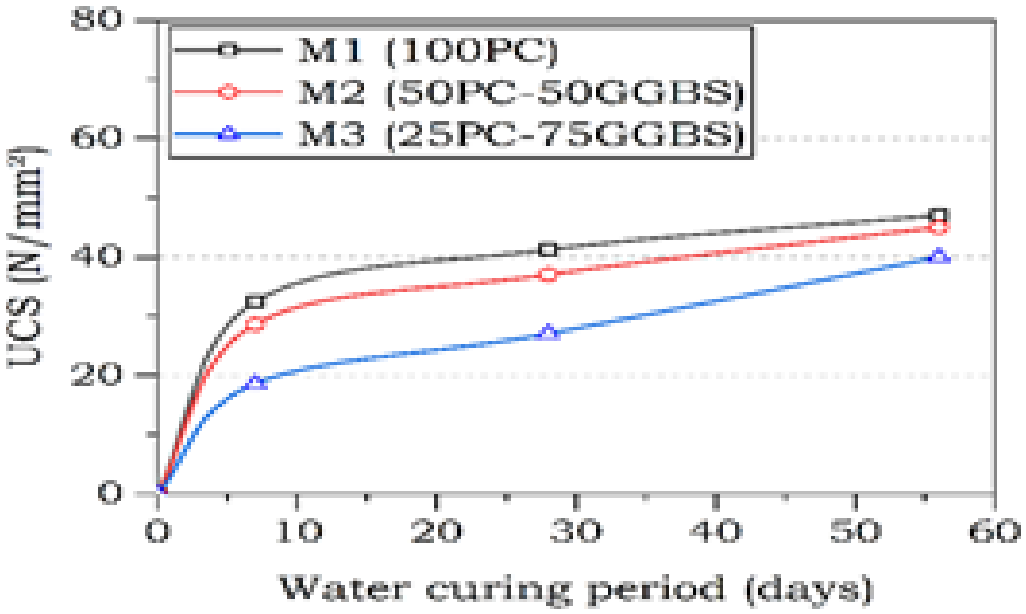

Fig 4: Unconfined compression strength development of water-cured concrete.

Generally, a steady increase in the UCS was observed for all the concretes cured in water, demonstrating the formation of new hydrates, and confirming that the strength of cubes followed the general trend of UCS development. This strength development is owing to the initial hydration of cement components with water to produce hydrated products (calcium silicate hydrate; CSH and calcium aluminate hydrate; CAH), which are responsible for the densification of the concrete system [2].

The effect of the use of GGBS observed in M2 and M3 showed that there was a steady decrease in the UCS value at all the curing ages, as the quantity of GGBS increases. However, such a strength reduction was more pronounced at the early curing age (7 and 28 days) and was also in agreement with the consensus among engineering researchers [30]. The strength reduction associated with the incorporation of GGBS at the early age (7 and 28 days) is due to; 1) the lower calcium oxide within the GGBS-based system; 2) the slow hydration reactivity of GGBS, as the GGBS is a latent hydraulic binder providing minimal hydration; and 3) the delay of the hydration reaction resulting in the retardation of the setting time of GGBS-based concrete, relative to PC-based concrete [31]. As for the strength enhancement of GGBS-based concrete at the later curing age (56 days) is probably due to the higher alumina oxide and silicon oxide released from the dissolution of GGBS. These dissolved products lead to the formation of further hydrated products (pozzolanic products). The additional hydrates fill the pore spaces, thereby densifying and interlocking the system, and inducing a more compacted concrete structure, all of which induces a UCS improvement [31,32].

2.2- TSS of concretes cured in water

The tensile splitting strength (TSS) is an essential parameter for indicating the behavior of the formulated concrete mixes to crack development, shear failure, steel anchorage and other applications in hardened concrete. **Fig. 5** shows the variation in the TSS of all the formulated concrete mixes at the end of 28 days of an ambient curing period in water.

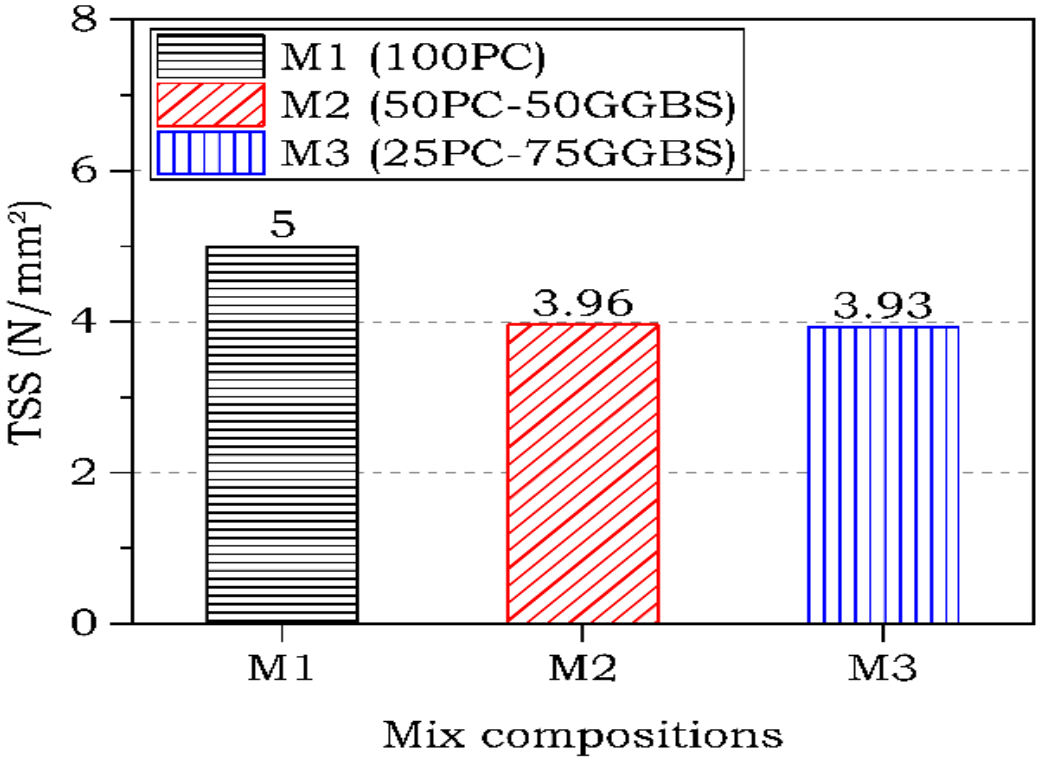

Fig. 5: 28-day-TSS of hardened concretes.

Like the UCS, the result showed that the 28-day-TSS of concrete mixes was adversely affected by the inclusion of GGBS. This was evident from the **Fig.5**, as the TSS was reduced from 5 N/mm^2 (for M1: 100PC) to 3.96 N/mm^2 (for M2: 50PC-50GGBS) and then to 3.93 N/mm^2 (M3: 25PC-75GGBS), when 50% and 75% of the cement content was replaced with GGBS, respectively. A similar decreasing trend in TSS was reported by other researchers [33–38], who attribute the TSS reduction to the inadequate interfacial transition zone bond between the cement matrix and the aggregates at the early curing age. Mo et al., [36] also pointed out that the incorporation of GGBS as a higher cement replacement level (60%) yielded a poorer adhesion with steel fibers, reducing the beneficial impact of steel fibers on the tensile splitting strength of oil palm shell concrete containing GGBS.

3- Strength development in sulfate solution

3.1-UCS of concretes cured in sulfate

The UCS development of all the formulated concretes cured in a hybrid sulfate solution of sodium sulfate and magnesium sulfate over a prolonged curing period of up to 56 days, is depicted in **Fig. 6**, along with their water-cured counterparts for comparison.

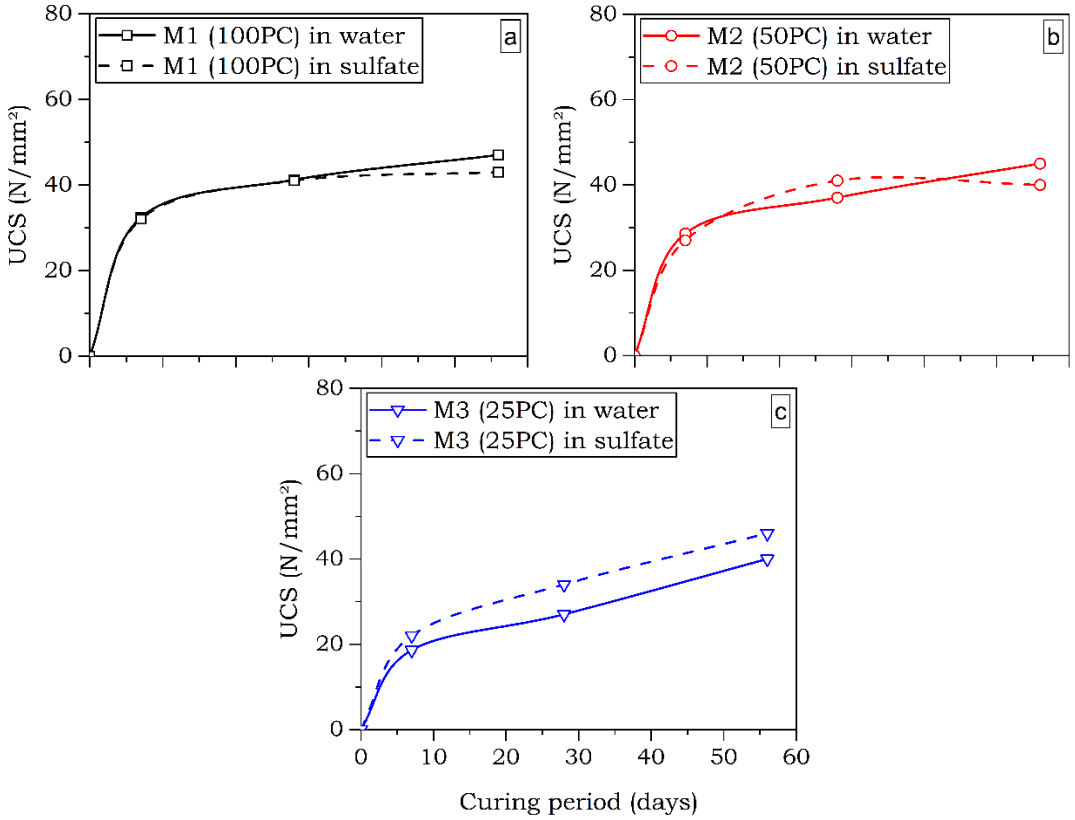

Fig. 6: UCS development of water and sulfate-cured concrete specimens.

In general, the observation indicated that the effect of binary sulfate solution on the UCS performance is proportional to both the curing period and the binder composition. In the case of the control mix (M1: 100PC), the result revealed a strength reduction in the range of 1 to 5 N/mm^2, and such a reduction was more noticeable at 56-days curing in sulfate, where the UCS was reduced from 47.5 to 43 N/mm^2. This deteriorative strength could be credited to the interaction between the sulfate and hydrated products of cement, which forms a series of topochemical interactions [39], mainly gypsum and then ettringite, of which the growth of the latter leads to cracks and expansion of the host matrix [40-41]. Briefly, in the presence of sulfate in concrete, the first reaction that takes place is the formation of gypsum. This typically occurred as a result of three main reactions; mainly due to; 1) the reaction between the calcium ions released from the cement hydration and the sulfate ions released through the ionic dissociation of magnesium and sodium sulfate [42]; 2) the reaction between the sulfate and the formed calcium silicate hydrate (CSH) [39,43]; and 3) the reaction between the portlandite (calcium hydroxide) formed during the cement hydration and the penetrated sulfate [39]. Whatever the origin of gypsum formation, these formed minerals have been associated with softening (strength reduction) of the concrete and maximizing the volume of hardened concrete structure [44,45]. Additionally, the formed gypsum minerals can react with non-hydrated and hydrated calcium aluminate compounds (such as hydrated calcium aluminate; C_4AH_{13}, mono-sulfate; $C_4A\bar{S}H_{12\text{-}18}$, hydro-garnet; C_3AH_6, and non-hydrated tricalcium aluminate; C_3A) to form an additional secondary ettringite ($C_6A\bar{S}H_{32}$). The non-hydrated tricalcium aluminate and mono-sulfate can also react with sodium sulfate to form additional ettringite [43]. This formed mineral (ettringite) is a hydrous calcium aluminate sulfate mineral, growing typically as needle or rod-shaped crystals in the pore spaces of the

concrete, and having higher water absorption capability. These highly hydrated crystalline minerals (ettringite) have a higher specific surface area with unbalanced surface charges, so they inflict bipolar water molecules attraction [9,10], and hence, the orientation of water molecules to mitigate their surface energy. This, therefore, builds up a water layer around the surface of ettringite, which in turn densifies the concrete pores.

Once the volume of the ettringite exceeds the volume of concrete pores, the further continuous growth of ettringite then generates internal stress, expressing a gap between the ettringite crystals and hydrated gel [14,45,46]. This is typically followed by the appearance of cracks and expansion of the host concrete matrix once the generated stress exceeds the tensile strength. Subsequently, a concrete UCS deterioration cooccurred [43,47], which was also in support of why the UCS of M1: 100PC cured in sulfate reduced relative to their water-cured counterparts.

Conversely, a slight strength gain was recorded for the UCS of M2: 50PC-50GGBS at the end of 28 days, where the mix experienced a higher UCS value of 42 N/mm^2 in sulfate, relative to its water-cured counterpart of 38 N/mm^2. This, however, was not the case for the M3: 25PC-75GGBS, as the strength observation exhibited a strength gain in the range of 4-to-8 N/mm^2 at all the curing ages. The strength gain associated with the incorporation of GGBS is possibly attributed to the lower quantity of portlandite produced during the cement hydration, the lower Al_2O_3 of the GGBS and the reduction of non-hydrated tricalcium aluminate (C_3A) of the binder, all of which reduce the formation of ettringite. Therefore, the concrete pores were probably enough for the nucleation and growth of the ettringite in the case of M2 up to 28 days, before such a growth exerts pressure on the surrounding hydrated gels, thus, causing cracks and a strength reduction at the end of 56 days. This explanation is also in line with the observation of M3: 25PC-75GGBS due to the further reduction in the quantity of portlandite, the quantity of non-hydrated tricalcium aluminate, and the quantity of Al_2O_3, all of which induce a small amount of ettringite, which was also in line with the X-ray diffraction pattern of several publications [7].

3.1-TSS of concretes cured in sulfate

The representative TSS values of all the concrete cylinders cured in a binary sulfate solution of sodium and magnesium sulfate over a curing period of 28 days are illustrated in **Fig.7**, alongside their water-cured counterparts as references.

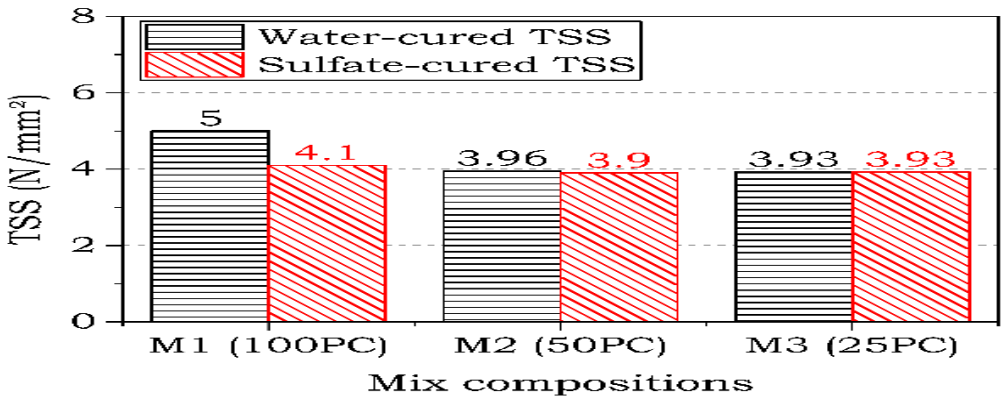

Fig.7: 28-day-TSS of concrete specimens cured in water and sulfate.

Like the case of UCS, the TSS observation indicated that the effect of sulfate on concrete is proportional to GGBS content in the mix. The control mix (M1), which was fabricated using cement only, suffered considerably from sulfate, where the 28-day-TSS value was reduced from 5 N/mm^2 to 4.1 N/mm^2, accounting for a 0.9 N/mm^2 reduction in the TSS due to exposure to sulfate attack. On the contrary, only a TSS reduction of 0.1 and 0 N/mm^2 was monitored when 50% and 75% cement substitution percentage with GGBS was utilized, respectively. This, therefore, suggests the beneficial impact of GGBS on the residual TSS of concrete after exposure to sulfate attack, particularly at a higher cement substitution level (75%). This improvement in TSS can be credited to the lower quantity of portlandite, the lower Al_2O_3, and the reduction of non-hydrated tricalcium aluminate (C_3A) of the GGBS-based concrete matrix, all of which reduce the ettringite, thus eliminating the crack formation and concrete deterioration.

Conclusion

The main conclusions can be drawn as follows:

The use of GGBS as a partial cement substation experienced an increase in the consistency of concrete due to the poorer early hydration, the lower calcium oxide, and the lower water absorption of the GGBS-based system.

Under the water curing condition, the UCS results of concrete revealed a reduction in the UCS as the GGBS content increases, at the early curing ages (7 and 28 days), due to the reduction in calcium oxide and the delay of the hydration. However, such a UCS reduction was compensated at 56 days, particularly for M2 (50PC-50GGBS), due to the formation of further hydrated products, which densifies the structure and thus improves the UCS.

The exposure of PC-based concrete to a sulfate solution of magnesium and sodium sulfate induces a reduction in the UCS and TSS at all the curing ages, due to the growth of ettringite.

The use of GGBS as a cement substitution yielded a superior sulfate resistance, as the retained UCS and TSS of GGBS-based concrete after the immersion in sulfate solution, was higher than the strength of PC-based concrete. This superiority is attributed to the lower portlandite content, the lower Al_2O_3, and the reduced non-hydrated tricalcium aluminate (C_3A), which restricts the ettringite formation.

The limitations to this research study, which could have an impact on the authenticity of the experimentation outcomes, are the use of a single concentration of hybrid sulfate solution of magnesium sulfate and sodium sulfate, and the use of single grade of GGBS. Hence, a research studies considering the effect of different sulfate combinations and different GGBS grads, are advised for future work to overcome this deficiency.

Overall, the feasibility of developing a sustainable concrete capable of restricting sulfate attack by using GGBS as a partial cement substitution, has been confirmed in this research study. This finding may have some bearing on the current practices, and relevant to all the civil engineers who are involved in concrete technology, as this document will serve as an invaluable resource of in-depth and up-to-date information on the use of GGBS as a partial replacement of cement. The application of this type of concrete is also anticipated to alleviate the soci-economic and environmental concerns

associated with the manufacturing of Portland cement, as it will reduce the total carbon dioxide emissions and the intensive energy consumption associated with concrete.

References

[1] Abdalla, T.A., Koteng, D.O., Shitote, S.M., and Matallah, M., (2022), Mechanical and durability properties of concrete incorporating silica fume and a high volume of sugarcane bagasse ash., Results in Engineering., **16**, 100666. DOI: 10.1016/j.rineng.2022.100666.

[2] Adeleke, B.O., Kinuthia, J.M., Oti, J., and Ebailila, M., (2023), Physico-mechanical evaluation of geopolymer concrete activated by sodium hydroxide and silica fume-synthesised sodium silicate solution., Materials., **16**(6), 2400. DOI: 10.3390/ma16062400.

[3] Nukah, P.D., Abbey, S.J., Booth, C.A., and Oti, J., (2022), Evaluation of the structural performance of low carbon concrete., Sustainability., **14**(24), 16765. DOI: 10.3390/su142416765.

[4] Samad, S., Shah, A., and Limbachiya, M.C., (2017), Strength development characteristics of concrete produced with blended cement using ground granulated blast furnace slag (GGBS) under various curing conditions., Sadhana - Academy Proceedings in Engineering Sciences., **42**, 1203-121342. DOI: 10.1007/s12046-017-0667-z.

[5] Oti, J.E., Kinuthia, J.M., and Bai, J., (2009), Compressive strength and microstructural analysis of unfired clay masonry bricks., Engineering Geology., **109**(3-4), 230-240. DOI: 10.1016/j.enggeo.2009.08.010.

[6] Dave, N., Misra, A.K., Srivastava, A., and Kaushik, S.K., (2016), Experimental analysis of strength and durability properties of quaternary cement binder and mortar., Construction and Building Materials., **107**, 117-124. DOI: 10.1016/j.conbuildmat.2015.12.195.

[7] Yan, X., Jiang, L., Guo, M., Chen, Y., Song, Z., and Bian, R., (2019), Evaluation of sulfate resistance of slag contained concrete under steam curing., Construction and Building Materials., **195**, 231-237. DOI: 10.1016/j.conbuildmat.2018.11.073.

[8] Ogawa, S., Nozaki, T., Yamada, K., Hirao, H., and Hooton, R.D., (2012), Improvement on sulfate resistance of blended cement with high alumina slag., Cement and Concrete Research, **42**(2), 244-251. DOI: 10.1016/j.cemconres.2011.09.008.

[9] Ebailila, M., Kinuthia, J., Oti, J., and Al-Waked, Q., (2022), Sulfate soil stabilisation with binary blends of lime–silica fume and lime–ground granulated blast furnace slag., Transportation Geotechnics., **37**, 100888. DOI: 10.1016/j.trgeo.2022.100888.

[10] Ebailila, M., Kinuthia, J., and Oti, J., (2022), Suppression of Sulfate-Induced Expansion with Lime–Silica Fume Blends., Materials., **15**, 2821. DOI: 10.3390/ma15082821.

[11] Mehta, A., and Ashish, D.K., (2020), Silica fume and waste glass in cement concrete production: A review., Journal of Building Engineering., **29**, 100888. DOI: 10.1016/j.jobe.2019.100888.

[12] Johari, M.M., Brooks, J.J., Kabir, S., and Rivard, P., (2011), Influence of supplementary cementitious materials on engineering properties of high strength concrete., Construction and Building Materials., **25**, 2639-2648. DOI: 10.1016/j.conbuildmat.2010.12.013.

[13] Hadjsadok, A., Kenai, S., Courard, L., Michel, F., and Khatib, J., (2012), Durability of mortar and concretes containing slag with low hydraulic activity., Cement and Concrete Composites, **34**(5), 671-677. DOI: 10.1016/j.cemconcomp.2012.02.011.

[14] El-Hachem, R., Rozière, E., Grondin, F., and Loukili, A., (2012), Multi-criteria analysis of the mechanism of degradation of Portland cement based mortars exposed to external sulphate attack., Cement and Concrete Research., **42**(10), 1327-1335. DOI: 10.1016/j.cemconres.2012.06.005.

[15] Zhang, M., Chen, J., Lv, Y., Wang, D., and Ye, J., (2013), Study on the expansion of concrete under attack of sulfate and sulfate–chloride ions., Construction and Building Materials, **39**, 26-32. DOI: 10.1016/j.conbuildmat.2012.05.003.

[16] BS EN 197-1:2011, Cement — Part 1: Composition, specifications and conformity criteria for common cements, BSI Standards Limited, London, UK, 2011. https://doi.org/10.3403/30205527.

[17] BS EN 15167-1:2006, Ground granulated blastfurnace slag for use in concrete, mortar and grout—Part 1: definitions, specifications and conformity criteria, BSI Standards Limited, London, UK, 2006. https://doi.org/10.3403/30130594.

[18] BS EN 12620:2002+A1:2008, Aggregates for concrete, BSI Standards Limited, London, UK, 2008. https://doi.org/10.3403/02661981.

[19] BS EN 206:2013+A2:2021, Concrete — Specification, performance, production and conformity., BSI Standards Limited, London, UK, 2021. https://doi.org/10.3403/30257890.

[20] BS EN 12350-1:2019, Testing fresh concrete—Part 1: Sampling and common apparatus, BSI Standards Limited, London, UK, 2019. https://doi.org/10.3403/30360061.

[21] BS EN 12390-1: 2021, Testing hardened concrete—Part 1: Shape, dimensions and other requirements for specimens and moulds, BSI Standards Limited, London, UK, 2021. https://doi.org/10.3403/30397529U.

[22] BS EN 12350-2: 2019, Testing fresh concrete — Part 2: Slump test, BSI Standards Limited, London, UK, 2019. https://doi.org/10.3403/30360058.

[23] BS EN 12350-4: 2019, Testing fresh concrete — Part 4: Degree of compactability, BSI Standards Limited, London, UK, 2019. https://doi.org/10.3403/30360064.

[24] BS EN 12390-3:2019, Testing hardened concrete — Part 3: Compressive strength of test specimens, BSI Standards Limited, London, UK, 2019. https://doi.org/10.3403/30360070.

[25] BS EN 12390-6:2009, Testing hardened concrete — Part 6: Tensile splitting strength of test specimens, BSI Standards Limited, London, UK, 2009. https://doi.org/10.3403/30200045.

[26] Gu, P., Beaudoin, J.J., Zhang, M.H., and Malhotra, V.M., (2000), Performance of reinforcing steel in concrete containing silica fume and blast-furnace slag ponded with sodium chloride solution., ACI Materials Journal., **97**(3), 254-262. DOI: 10.14359/4620.

[27] Park, C.K., Noh, M.H., and Park, T.H., (2005), Rheological properties of cementitious materials containing mineral admixtures., Cement and concrete research., **35**(5), 842-849. DOI: 10.1016/J.CEMCONRES.2004.11.002.

[28] Teng, S., Lim, T.Y.D., and Divsholi, B.S., (2013), Durability and mechanical properties of high strength concrete incorporating ultra fine ground granulated blast-furnace slag., Construction and Building Materials., **40**, 875-881. DOI: 10.1016/J.CONBUILDMAT.2012.11.052.

[29] Bostancı, Ş.C., Limbachiya, M., and Kew, H., (2016), Portland slag and composites cement concretes: engineering and durability properties., Journal of Cleaner Production., **112**, 542-552. DOI: 10.1016/J.JCLEPRO.2015.08.070.

[30] Özbay, E., Erdemir, M. and Durmuş, H.İ., 2016), Utilization and efficiency of ground granulated blast furnace slag on concrete properties–A review., Construction and Building Materials., **105**, 423-434. DOI: 10.1016/J.CONBUILDMAT.2015.12.153.

[31] Mo, K.H., Ling, T.C., Alengaram, U.J., Yap, S.P., and Yuen, C.W., (2017), Overview of supplementary cementitious materials usage in lightweight aggregate concrete., Construction and Building Materials., **139**, 403-418. DOI: 10.1016/J.CONBUILDMAT.2017.02.081.

[32] Gholampour, A., and Ozbakkaloglu, T., (2017), Performance of sustainable concretes containing very high volume Class-F fly ash and ground granulated blast furnace slag., Journal of Cleaner Production., **162**, 1407-1417. DOI: 10.1016/J.JCLEPRO.2017.06.087.

[33] Türkmen, İ., and Fındık, S.B., (2013), Several properties of mineral admixtured lightweight mortars at elevated temperatures., Fire and materials, **37**(5), 337-349. DOI: 10.1002/FAM.1030.

[34] Mo, K.H., Alengaram, U.J., Jumaat, M.Z., and Yap, S.P., (2015), Feasibility study of high volume slag as cement replacement for sustainable structural lightweight oil palm shell concrete., Journal of cleaner production., **91**, 297-304. DOI: 10.1016/J.JCLEPRO.2014.12.021.

[35] Mo, K.H., Alengaram, U.J., and Jumaat, M.Z., (2015), Utilization of ground granulated blast furnace slag as partial cement replacement in lightweight oil palm shell concrete., Materials and structures., **48**, 2545-2556. DOI: 10.1617/S11527-014-0336-1/METRICS.

[36] Mo, K.H., Chin, T.S., Alengaram, U.J., and Jumaat, M.Z., (2016), Material and structural properties of waste-oil palm shell concrete incorporating ground granulated blast-furnace slag reinforced with low-volume steel fibres., Journal of Cleaner Production., **133**, 414-426. DOI: 10.1016/J.JCLEPRO.2016.05.162.

[37] Sekar, S.K., (2016), Mechanical and fracture characteristics of Eco-friendly concrete produced using coconut shell, ground granulated blast furnace slag and manufactured sand., Construction and Building Materials., **103**, 1-7. DOI: 10.1016/J.CONBUILDMAT.2015.11.035.

[38] Jayaprithika, A., and Sekar, S.K., (2016), Stress-strain characteristics and flexural behaviour of reinforced Eco-friendly coconut shell concrete., Construction and Building Materials., **117**, 244-250. DOI: 10.1016/J.CONBUILDMAT.2016.05.016.

[39] Cefis, N., and Comi, C., (2017), Chemo-mechanical modelling of the external sulfate attack in concrete. Cement and Concrete Research, **93**, 57-70. DOI: 10.1016/J.CEMCONRES.2016.12.003.

[40] Ebailila, M., Kinuthia, J., and Oti, J., (2022), Role of Gypsum Content on the Long-Term Performance of Lime-Stabilised Soil., Materials., **15**(15), 5099. DOI: 10.3390/ma15155099.

[41] M. Ebailila, Sulfate soil stabilisation with silica fume-based binders, Doctoral Thesis, University of South Wales, England, UK, 2022.

[42] Sun, D., Wu, K., Shi, H., Miramini, S., and Zhang, L., (2019), Deformation behaviour of concrete materials under the sulfate attack., Construction and Building Materials., **210**, 232-241. DOI: 10.1016/J.CONBUILDMAT.2019.03.050.

[43] Sarkar, S., Mahadevan, S., Meeussen, J.C.L., Van der Sloot, H., and Kosson, D.S., (2010), Numerical simulation of cementitious materials degradation under external sulfate attack., Cement and Concrete Composites., **32**(3), 241-252. DOI: 10.1016/J.CEMCONCOMP.2009.12.005.

[44] Santhanam, M., Cohen, M.D., and Olek, J., (2003), Effects of gypsum formation on the performance of cement mortars during external sulfate attack., Cement and concrete research., **33**(3), 325-332. DOI: 10.1016/S0008-8846(02)00955-9.

[45] Rahman, M.M., and Bassuoni, M.T., (2014), Thaumasite sulfate attack on concrete: Mechanisms, influential factors and mitigation., Construction and Building Materials., **73**, 652-662. DOI: 10.1016/J.CONBUILDMAT.2014.09.034.

[46] Tian, B., and Cohen, M.D., (2000), Does gypsum formation during sulfate attack on concrete lead to expansion?., Cement and concrete research., **30**(1), 117-123. DOI: 10.1016/S0008-8846(99)00211-2.

[47] Sun, C., Chen, J., Zhu, J., Zhang, M., and Ye, J., (2013), A new diffusion model of sulfate ions in concrete., Construction and Building Materials., **39**, 39-45. DOI: 10.1016/J.CONBUILDMAT.2012.05.022.